1-1-2016

Impedance-Based Water-Quality Monitoring Using the Parallel-Plate Method

Ali Nazari
Boise State University

Arvin Farid
Boise State University

Ken Cornell
Boise State University

doi: 10.1061/9780784480151.038

IMPEDANCE-BASED WATER-QUALITY MONITORING USING PARALLEL-PLATE METHOD

Ali Nazari[1], Arvin Farid[2], and Ken Cornell[3]

[1]Master of Geotechnical Engineering , Department of Civil Engineering, Boise State University, 1910 University Drive, MS 2060, Boise, ID 83725-2060
[2]Associate Professor, Department of Civil Engineering, Boise State University, 1910 University Drive, MS 2060, Boise, ID 83725-2060
[3]Associate Professor, Department of Chemistry and Biochemistry, Boise State University, 1910 University Drive, MS 1520, Boise, ID 83725-1520

ABSTRACT: The application of electromagnetic (EM) waves to measure the electrical properties (dielectric constant and loss tangent) of materials is a well-known approach. The electrical properties can be used to indirectly measure several physical properties of solutions in water such as the concentration and chemical composition of contaminants in water, as a representative of the liquid phase in soil. A capacitive method of measuring dielectric properties of solutions is proposed to detect and determine low-concentration chemical and biological contaminations in water. The primary objective of this project is to design a low-cost sensor that would require small volumes of samples to detect low concentrations of dissolved contaminants in water. A forward model was developed using a finite-element method (FEM) to simulate the experimental setup (EXP). A calibration function was also developed to minimize deviations between FEM and EXP results for benchmark/reference solutions with known dielectric properties. The validated, calibrated forward model was then inverted to calculate the electrical properties of unknown solutions using the corresponding EXP results.

INTRODUCTION

Water quality is a growing concern among state and federal agencies in the nation and among the public. Contamination of groundwater is also a subject of national importance because groundwater is used for drinking water by about 50% of the nation's population (U.S.G.S., 2012). An example of possible contaminants in water is salts in groundwater and surface-water reservoirs near roads. These water resources are threatened by deicing agents such as sodium or magnesium chloride during winter snow-storm seasons as well as being a major constituent of waste water produced during oil and gas production. The waste water or brine needs to be treated and/or disposed of, providing a daily challenge for operators and resource managers. Some elements of salts are regulated, with water-

quality criteria established for the protection of aquatic wildlife. For instance, chloride (Cl–) has an acute standard of 860 mg/L or 0.024 Molar (Farag and Harper, 2014).

Each solution has a unique set of electrical characteristics governed by its electrical (dielectric constant and electrical conductivity) properties. Thus, the knowledge of the dielectric constant and electrical conductivity of solutions enables tracing changes in the concentration of contaminants to discriminate water from contaminated water. To measure the dielectric constant of a medium, a reflectometric method can be applied. The reflectometric method is described as measuring the reflection response of a medium over the microwave frequency (915 MHz to 2450 MHz) at the interface of the medium and a wave port (Komarov et al., 2005). The results are then linked to the dielectric properties of the medium.

The dielectric property of a material is an expression of the material's interaction with electromagnetic fields. Complex-relative dielectric permittivity (ε_r^*) is the complex dielectric permittivity (ε^*) normalized to that of free space ($\varepsilon_0 = 8.8541878176 \times 10^{-12}$ *F/m*) defined as:

$$\varepsilon_r^* = \varepsilon_r' - j\varepsilon_r'' \quad (1)$$

where $j = \sqrt{-1}$; ε_r' is the real part of the complex relative dielectric permittivity (also known as the dielectric constant), and ε_r'' is the imaginary part of the complex relative dielectric permittivity (referred to as the loss factor). The ratio between the dielectric constant (ε_r') and the loss factor (ε_r'') corresponds to the dissipation factor or loss tangent ($\tan\delta$). Electrical conductivity (σ) is another important electrical property, which measures the ability of materials to conduct an electric current.

Dielectric-measurement methods depend on both physical and electrical natures of the dielectric material being measured, the frequency of interest, and the required degree of accuracy. Referring to a comparison among common dielectric-measuring techniques table in Jilani et al., 2012, for the purpose of this work, the parallel-plate (capacitive) method is determined to be the suitable technique because of the ability of the method to preserve the sensitivity and reduce the setup dimensions.

In this method, the metallic plates are coated with a dielectric material to prevent any electrical contact between the sample and the measurement conductive plates. Parallel-plate systems use a parallel-plate capacitor as a sample holder, with the material under testing (MUT) sandwiched between the plates of the capacitor. After placing a sample into the parallel-plate sample holder, a capacitor is formed. This method requires an impedance analyzer or LCR-meter (inductor, capacitor, resistor meter). The MUT is stimulated by an alternating current (AC) source, and the actual voltage across the material is monitored. The MUT's test parameters are derived from the dimensions of the material and measuring its capacitance and dissipation factor. The measured capacitance is then used to calculate the MUT's dielectric permittivity. This method is common at a wide frequency range, typically below 1 GHz and has high ε_r' measurement accuracy, usually ±1%. However, air gaps between the sample and capacitor plates can cause significant errors, if not accounted for and calibrated for (Tereshchenko, 2011). In addition, due to the electrode-polarization effect, spurious measurements lead to poor results. This can be mitigated using electrodes with a large surface area compared to their thickness or at higher frequencies, as the effect is reduced rapidly with increasing frequency (Jilani et al., 2012).

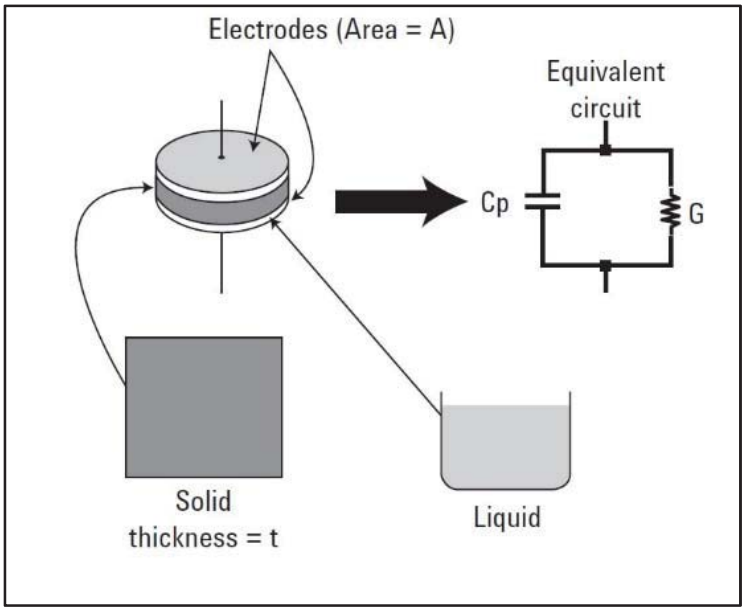

Figure 1. Parallel-plate (capacitive) method (Agilent, 2008)

A transmission line (T-line) is an electrical-circuit element, i.e., a coaxial cable designed to carry electromagnetic waves with minimum loss. The load itself is considered a lumped element (i.e., small compared to a wavelength), and the wires connecting the T-line to the load are considered to be negligibly short. Wentworth (2005) states that, at $z = 0$,

$$V_0^- = \frac{Z_L - Z_0}{Z_L + Z_0} V_0^+ \quad (2)$$

where Z_L is the load impedance, Z_0 is the T-line impedance, and V_0^+ and V_0^- are the value of the $+z$ and $-z$ directed voltage waves, respectively at $z = 0^+$ and $z = 0^-$. Equation 2 states that if the characteristic impedance of the load is unequal to that of the line, then a portion of the EM wave's energy must be reflected at the load. The degree of the impedance mismatch is represented by the reflection coefficient at the load given by:

$$\Gamma_L = \frac{Z_L - Z_0}{Z_L + Z_0} = \frac{V_0^-}{V_0^+} \quad (3)$$

In the past 90 years, dielectric-measurement techniques have been developed as a tool for low-frequency characterization of samples to methods for extremely broadband spectroscopy and high-frequency imaging of materials (Kaatze, 2013). One concern in the history of dielectric-measurement techniques is the problem of measuring the liquid dielectric properties, which has practical applications in industrial and environmental fields. Blackham and Pollard (1997) presented an enhanced computational model for an open-ended coaxial probe used for dielectric permittivity measurement. Xie et al. (2004) estimated the electrical conductivity of brine water by measuring the electrical conductivity and dielectric permittivity of a mixture of brine water and other substances such as oil and gas. Jouyban et al. (2004) proposed a computational method for calculating dielectric constants of 30% to 70% volume fractions of solvents such as ethanol and propanol in water mixtures at fixed and/or various temperatures. They obtained a deviation less than 2% between the calculated and experimental dielectric constants (Jouyban et al., 2004). Peyman et al. (2007) measured the complex dielectric

permittivity of aqueous solutions at 20°C using an open-ended coaxial probe. The measurements were done over a range of frequency from 0.13 GHz to 20 GHz for various concentrations of NaCl solutions between 0.001 and 5 Molar. Lamkaouchi et al. (2003) used a free air transmission method at frequencies of 26 to 110 GHz to determine permittivity of lossy liquids such as water, NaCl solution with a salinity of 35%, and synthetic sea water. They measured the dielectric permittivity for a wide temperature range of −5 to 70°C. They improved the data that are incorporated in a number of microwave emissivity models used in numerical weather forecasting. Kheir et al. (2008) extracted the dielectric constant of liquids using a setup consisting of a microstrip-ring resonator covered with a metallic enclosure acting as a rectangular waveguide. They suggest that using both methods will definitely reduce the measurement ambiguity. Azad et al. (2013) and Bolvardi (2014) investigated the use of electromagnetic (EM) waves with various radiation patterns to induce a controlled transport of a nonhazardous dye (used as a contamination simulant). The medium in both studies was water, which helped monitoring the dye transport under EM stimulated conditions as well as in a porous medium. The results of the study suggested that dielectrophoresis could be the underlying mechanism behind the observed EM-induced dye flow in both aqueous and water-saturated porous media (Azad et al., 2013; Bolvardi, 2014).

METHODOLOGY

A new sensor, sensitive to minor changes in the concentration of dissolved material in water, was designed. The sensor was installed in an experimental (EXP) setup to observe the electromagnetic reflection response at the interface between a 50Ω wave-port and the interior medium of the EXP setup. The sensor is capable of examining various materials under test (MUTs). A forward numerical finite-element model using COMSOL Multiphysics® software was developed to numerically simulate the EXP setup and compute the reflection response of the medium. The forward model was thus used to compute the reflection response for reference solutions with known electrical and physical properties and calibrated against corresponding measurements. The calibrated forward model was then inverted to compute the dielectric constant, electrical conductivity, and in turn volumetric content of biological and chemical solutions.

Experimental Apparatus

A low-temperature co-fired ceramic (LTCC) system was employed to fabricate the initial sensor. In the design, an electrical circuit consisting of capacitor electrodes and connecting leads was embedded within ceramic sheets using a silver epoxy paste. The EM waves, emitted by a vector-network analyzer (VNA), propagating through an SMA (Subminiature Version A) connector, enter the target medium. The center line of the SMA connector is electrically connected to the top plate of the capacitor using connecting leads. The bottom plate of the capacitor was connected to the outer shield of the SMA connector, sharing the same ground with the VNA.

Capillary tubes were implemented for the insertion of the solution into the sensor. This minimized the introduction of air bubbles and their negative impact on measurements, lowered the signal-to-noise ratio, and enhanced the sensitivity of the setup. The use of capillary tubes provides the FEM-model with accurate dimensions.

Two series of biological and chemical solutions in water at different concentrations were prepared as MUTs (experimental samples). Sodium-chloride (NaCl) solution was selected as the chemical solution, since it is a common example of mineral contamination in water. Bovine serum albumin (BSA) protein was also selected as the biological solution in water. The reason behind the choice was the fact that BSA Protein Assay Standards are high-quality reference samples for generating accurate standard curves and calibration controls in total protein assays (Piercenet, 2014). BSA protein is also common due to its stability in biochemical reactions and low cost.

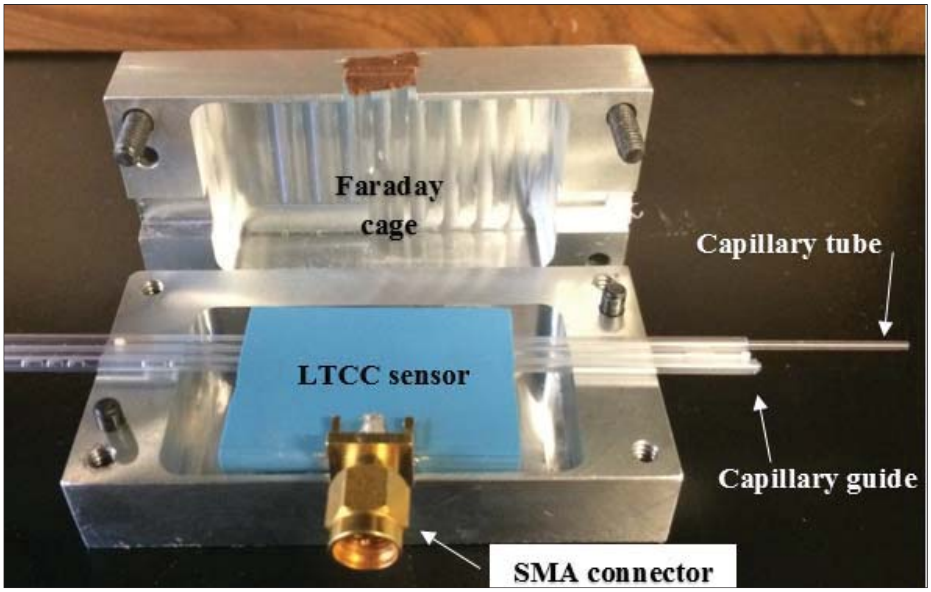

Figure 2. Final setup (disassembled)

Finite-Element Forward Model

The numerical (finite-element) forward model was used to simulated several samples with known dielectric properties. The model uses the known dielectric properties as inputs and computes the EM reflection response over the desired frequency range at the interface of the wave-port and the medium containing the sample. On the other hand, the reflection response for the same set of samples was obtained using the experimental setup. The first goal was to validate the FEM results against the EXP results.

The EXP and FEM results for liquid samples were compared, and their differences were recorded over the frequency range. The selected frequency range is narrow enough to allow the assumption that the dielectric properties variation is insignificant, and the materials are nondispersive. The dielectric properties of this kind of material are independent of the frequency variation as opposed to dispersive materials, whose dielectric properties are functions of frequency. This assumption disregards the dispersive nature of water and subsequently aqueous solutions.

Because it is computationally expensive to model all details of the real device, some details were simplified. Hence, there may be some discrepancies between the computed data and experimental measurements. A calibration function was developed to estimate the difference between FEM and EXP results for all the FEM results based on their

dielectric properties. This calibration function calibrates the FEM results and matches them best with EXP results. The calibrated FEM results were then used in the inverse model.

Inverse Model

For solutions with unknown electrical properties, the reflection response at the wave-port is measured using the experimental setup. The forward model is then inverted using an optimization scheme. The inverted model is referred to as the inverse model. The inverse model uses the EXP results (i.e., frequency-response measurements) as input. Then, the forward model is solved iteratively using various input electrical properties until an appropriate cost function (in this case, the difference between the numerical and experimental frequency responses for the unknown materials is minimized) to produce the dielectric properties of the unknown MUT.

SUMMARY OF RESULTS AND DISCUSSION

Experimental

The setup was tested for air over the wide frequency range of 1.0 - 7.6 GHz, completed in 5 steps. Based on the FEM results compared to the EXP results, the appropriate frequency range to verify the FEM data was between 3.0 GHz and 4.6 GHz. The error bars in these experiments were about 0.02 dB, which is as low as the VNA's calibration noise. The minimum reflection was observed where the difference was at its maximum among the samples with different concentrations. The minimum reflection occurs at the frequency where the impedance of the sensor filled with the MUT best matches the 50Ω impedance of the VNA. This frequency is obviously dependent on the MUT. This minimum reflection made it possible to discriminate one sample from another (Figure 3).

BSA samples were tested over the same frequency range of 3.0 - 4.6 GHz. The contrast among different concentrations of BSA solutions is smaller than the error bar of the measurement—which is as small as possible, i.e., the VNA's calibration error. In other words, this low signal/noise ratio makes it impossible to discriminate between the BSA samples (Figure 4) using this VNA, which is among the typical high-precision and high-accuracy VNAs in the market. This means a practical limit has been met. Hence, there is a need for other mechanisms to amplify the signal.

The reflection response of the BSA samples was also measured at higher frequencies, 4.5 - 6.1 GHz. According to Figure 5, the 1g/L BSA solution exhibits a considerable deviation from the distilled water benchmark over the frequency range of 5.0 - 5.5 GHz. The error bars remained at their minimum (the instrument's noise floor) as in the EXP results for the lower frequency range. The strongest contrast between the water benchmark and the 1g/L BSA sample occurs over the frequency range of 5.0 - 5.4 GHz. This is the best frequency range to discriminate BSA solutions from water. The magnitude of the error bars for BSA was close to the calibration error bar (0.02 dB) of the VNA. This result proves the error due to air bubbles has been eliminated at BSA samples.

FEM Forward Model

The FEM data agree reasonably with the EXP data at the frequency range of 3.0 - 4.6 GHz. The FEM data and EXP data do not agree well over other frequencies. One potential cause is the discrepancy in the geometry of the FEM model and the EXP setup.

Figure 3 includes both EXP and FEM data for all samples. It is noteworthy that the difference between the frequencies where the minimum reflections (i.e., best impedance-match frequencies) occurs in the FEM and EXP data is the same for all samples. This difference between the frequencies of minimum reflection is 60 MHz. This constant (60 MHz) shift (i.e., difference between the frequencies of minimum reflection) across all materials confirms that over the above-mentioned frequency range, the magnitude of the reflection depends solely on dielectric properties, and the best impedance-match frequency is influenced (shifted) by the geometry.

One of the two sets of the excreted data (FEM or EXP) needs to be shifted to match with the other one. All EXP data were, hence, shifted 60 MHz to the left of the frequency spectrum to synchronize with the FEM data to find the discrepancy for calibration purposes. This approach guarantees that the best impedance match occurs at the same frequency in both EXP and FEM data, and it compensates for the discrepancies due to the geometry (as mentioned, the geometry controls the best impedance-match frequency). FEM and EXP were then subtracted to show the trend of the deviation between them, which is needed to be calibrated out. According to Figure 3, the deviations between FEM and EXP data are almost constant except over the frequency range of 3.7 - 4.1 GHz. The changes in dielectric properties exhibit more impact on the frequency response over the same frequency range. The indicated frequency range was selected for the purpose of the optimization scheme used for solving the inverse problem. The differences between EXP and FEM results for water and 0.5M NaCl are used to logarithmically interpolate the difference between the FEM and EXP results corresponding to the dielectric properties of MUTs. The computed difference is added to the FEM frequency response to calibrate the FEM results to minimize the deviation between FEM and EXP results.

There are several justifications for the deviation between the FEM and the EXP data. These deviations are due to the discrepancies between the numerically simulated and actual geometry of the setup caused by defects in the LTCC fabrication process. The organic constituent of ceramic tapes burns during the procedure of laminating and co-firing the LTCC layers. Subsequently, the ceramic layers shrink down by the ratio of 0.8734, while the silver epoxy does not. This inconsistent shrinkage between the ceramic and silver epoxy causes minor deviations and inconsistencies in the sensor components' dimension and location. This issue makes it difficult to design and fabricate the sensor with high precision. On the other hand, the silver-epoxy trace diverges, and some silver particles penetrate into the LTCC layers at the vicinity of the silver-epoxy traces (Nair, 2013). The discontinuity of silver-epoxy particles produce conductive particles—with free charges—reradiating under EM excitation, leading to errors in frequency-response measurements. This phenomenon has a deteriorating effect on the accuracy of the measurement of the frequency response of the media.

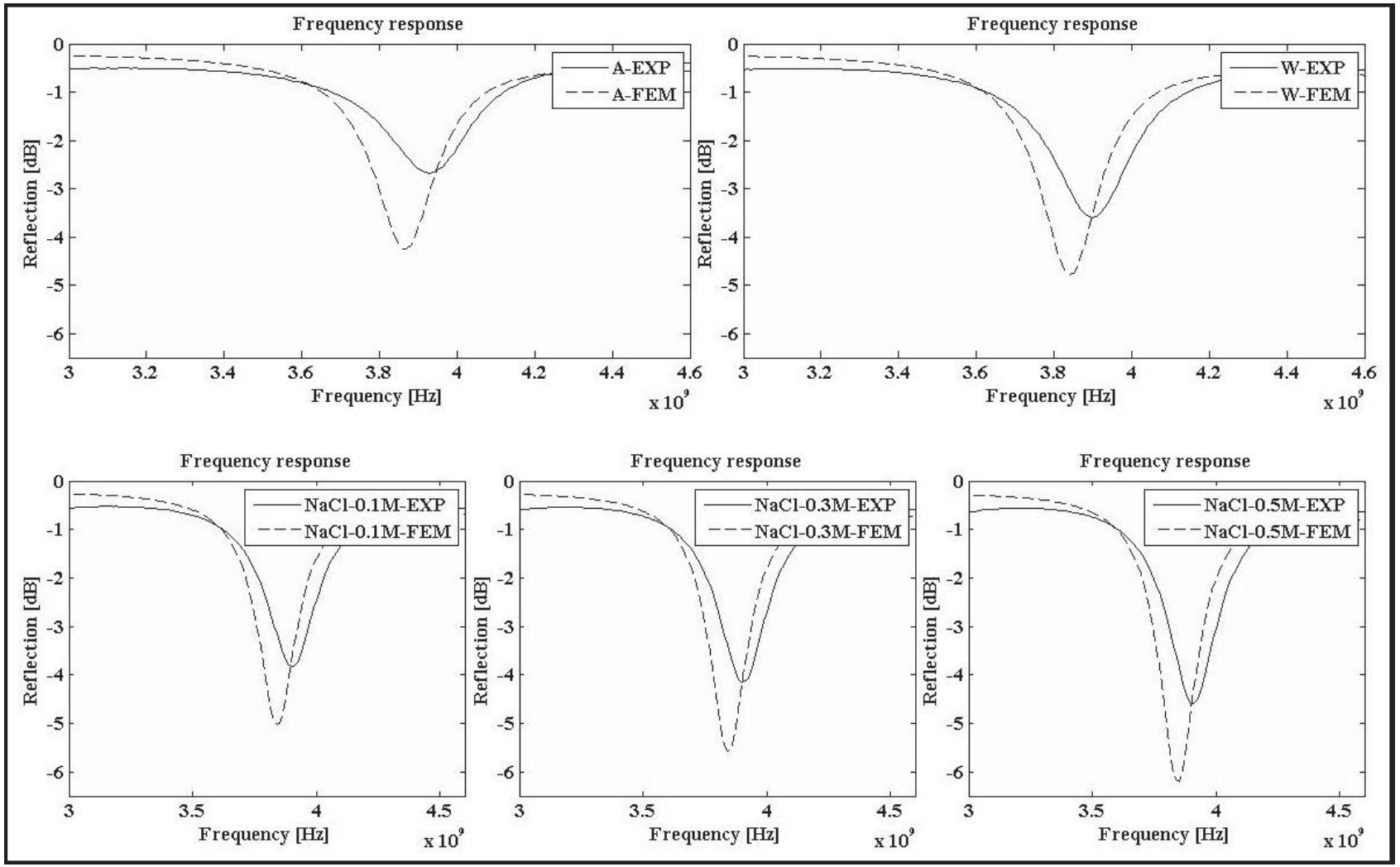

Figure 3. Comparison between FEM and EXP data of air (A), water (W), and NaCl samples of various concentrations for final setup

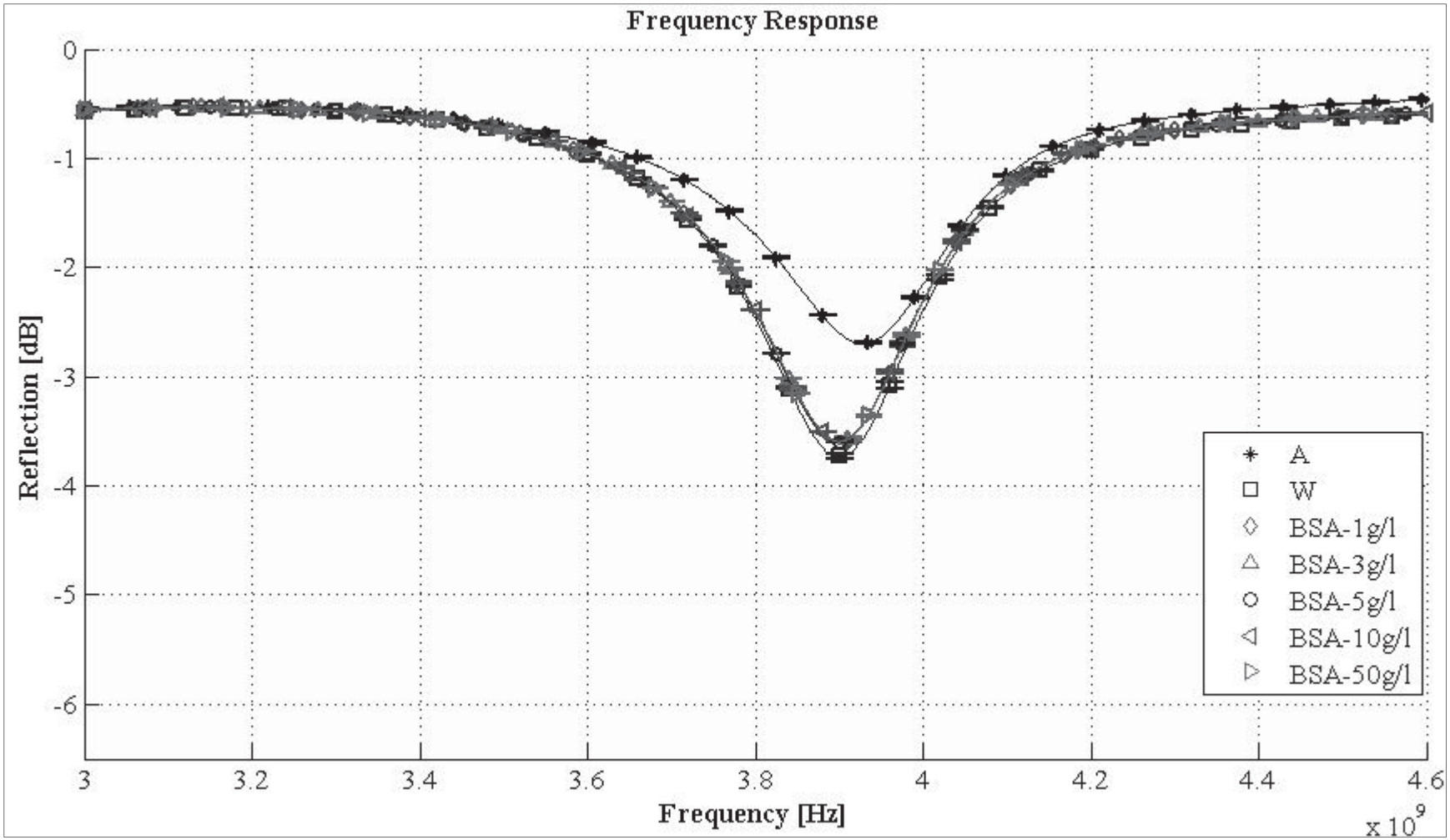

Figure 4. Frequency response of air (A), water (W), and BSAs of various concentrations for final setup

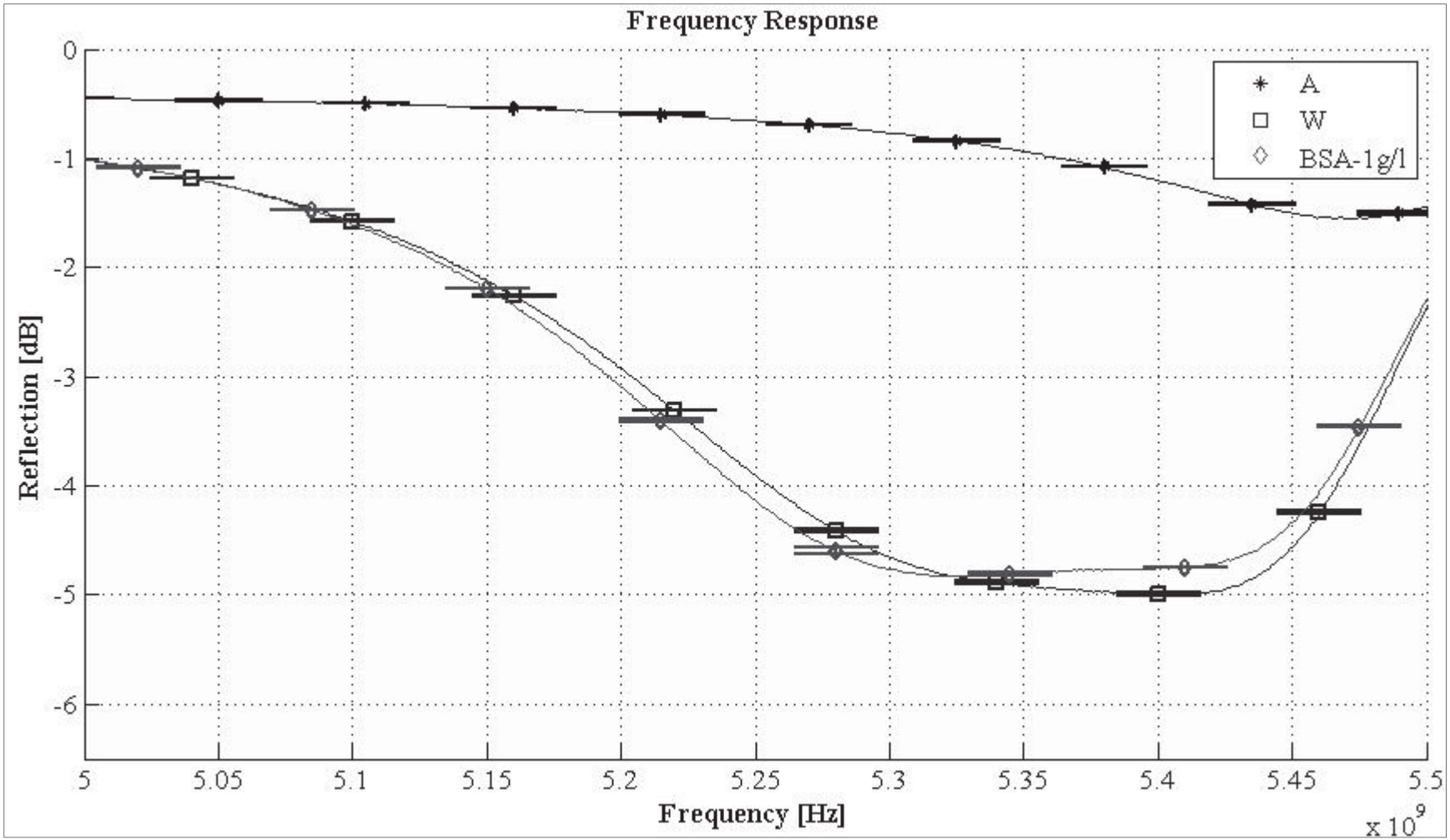

Figure 5. Frequency response of 1g/L BSA, air (A) and water (W) samples

Table 1. Example scenarios examined using the inverse model

Sample	Initial guess		Final estimate		Literature values*		RMSD [dB]	Absolute min [dB]	NRMSD [%]
	eps_r	Loss tan	eps_r	Loss tan	eps_r	Loss tan			
Air	1.0	0.00	1.000	0.0000	1.0	0.000	0.1204	2.6869	4.5%
Water	77.0	0.16	73.402	0.2077	76.7	0.157	0.0589	3.6095	1.6%
NaCl0.1M	77.0	0.16	70.611	0.3430	75.5	0.240	0.0663	3.8356	1.7%
NaCl0.3M	77.0	0.16	67.386	0.5185	69.3	0.435	0.0694	4.1607	1.7%
NaCl0.5M	77.0	0.16	62.685	0.7524	67.0	0.625	0.0751	4.6021	1.6%
BSA 50g/l	77.0	0.16	73.518	0.1758	N/A	N/A	0.0721	3.5339	2.0%

*Literature values are available at Von Hippel (1954)

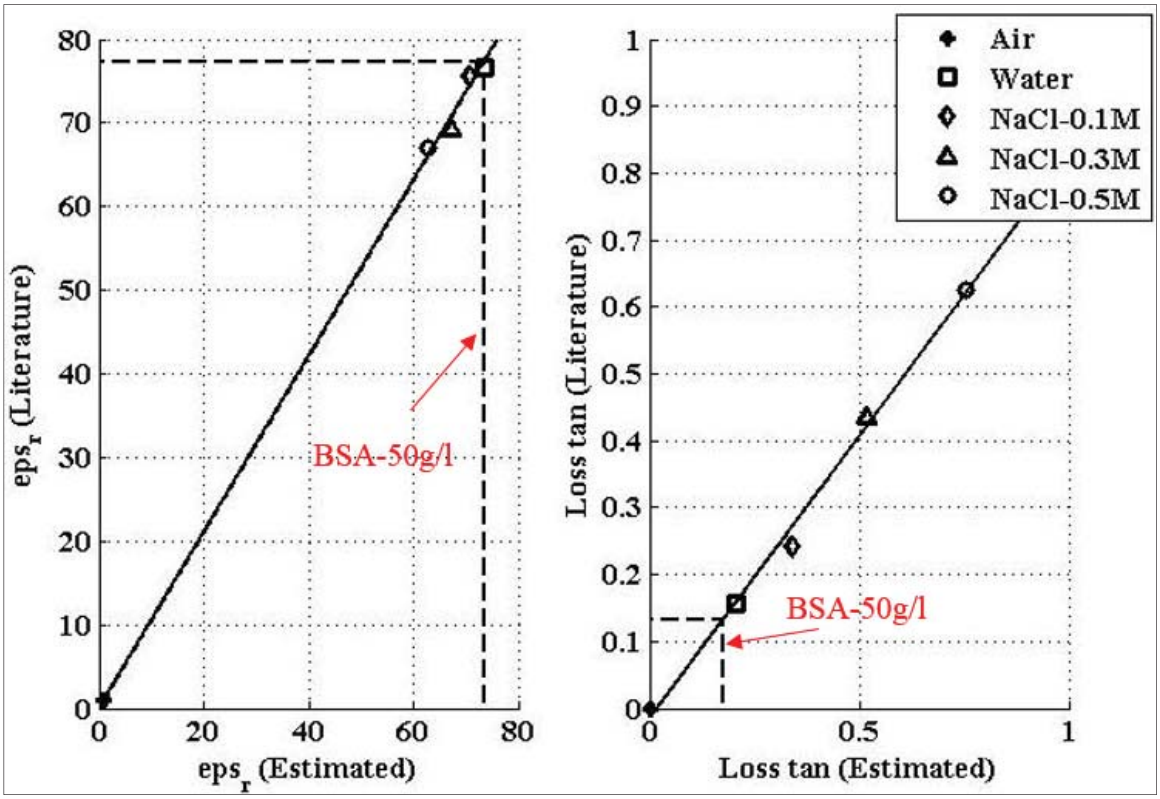

Figure 6. Calibrated values of dielectric properties for solutions in water

Inverse Model

The final results of eps_r and *loss-tan* of water along with all other samples are expressed in Table 1. An optimization scheme was simultaneously conducted for eight

data-points over the indicated frequency range at 0.1 GHz intervals. As shown in Table 1, there are differences between the computed dielectric properties and the literature values, particularly for water and 0.5M NaCl solution. These two samples were used as reference points to define the FEM model's calibration function; hence, their results should closely match with the literature values. The reason behind the choice of such values is that the INV (inverse) model attempts to optimize the reflection response at all of the eight frequency-points simultaneously, which results in an average RMSD at all eight frequency-points. Consequently, the dielectric properties corresponding to the minimum RMSD for water do not match with the literature values, which are used initially to develop the FEM forward model and its calibration function. In future studies, the optimization scheme should be conducted at each single frequency-point individually and followed with a set of dielectric properties at that frequency-point.

All scenarios are over the frequency range of 3.7 - 4.1 GHz. The result of the INV model suggests that as the concentration of NaCl samples and, in turn, the magnitude of the minimum reflection increase, the RMSD increases as well. The optimized dielectric properties of the samples in Table 1 are plotted in Figure 6 against properties available in the literature (refer to the "Materials and Methods" section). The data for eps_r follows a certain pattern. The *loss-tan* data follows a uniform trend. The equations of the trend line for the eps_r and the *loss-tan* are calculated using linear regression.

$$\varepsilon_{r-Literature} = 1.0522 \times \varepsilon_{r-Estimated} + 0.0123 \quad (4)$$

$R^2=0.9987$

$$tan(\delta)_{Literature} = 0.8429 \times \tan(\delta)_{Estimated} - 0.0157 \quad (5)$$

$R^2=0.9933$

Figure 6 shows the dielectric property data along with the lines that are fitted to them. Referring to the EXP data for BSA samples over the frequency range of 3.0 - 4.6 GHz, it is not possible to discriminate different concentrations of BSA. Yet the optimization scheme is conducted for the 50g/l BSA, and the derived dielectric properties are substituted in the calibration functions in Figure 6. The results are $eps_r = 77.3666$ and *loss-tan =0.1325*.

CONCLUSION

A new dielectric-measurement setup was developed, which is capable of detecting water-based biological or chemical mixtures in water at low concentrations. The setup includes a capillary sensor that requires quite small volumes of MUTs (0.9 cm^3) compared to other common methods in order to discriminate distilled water from contaminated water. This setup is useful for liquids only available in small quantities to monitor relatively low contamination levels. The dimensions of the sensor are small enough that it provides the compatibility to be embedded in small devices. The test procedure is reasonably simple and convenient to be mechanized. The air entrapment within samples, which is a common source of error in dielectric measurement for liquids, is avoided in this method. Using capillary tubes as sample holder makes it possible to inspect samples for possible entrapment of air before the measurements of the frequency response.

A numerical forward model was created to numerically simulate the experimental setup using an FEM method. The numerically simulated results for solutions of known dielectric properties in water were close to experimental results and followed the same

pattern and trend at specific ranges of frequency, but not at all frequencies. It is noteworthy that the precision in measuring the geometric dimensions of the setup to be input into the FEM forward model has a considerable influence on the FEM results. However, the numerical simulation of the setup at the current scale requires precise measurement of setup dimensions, which is impractical due to defects in the currently used sensor-fabrication process. The discrepancies between the EXP and FEM results were calibrated out.

An inverse model was developed over a specific frequency range of 3.7 - 4.1 GHz to utilize EXP data and FEM forward model to return dielectric properties of unknown solutions. The inverse-model results were not reliable due to their variation with respect to initial guesses input into the forward model. The results for high-concentration solutions in water were not at the desired level to be accepted. The explanation for these defects is the failure in perfectly verifying the initial forward model against experimental data over the entire frequency range. A thorough investigation is required to improve and calibrate precisely the forward model before subsequently applying the inverse model to make them applicable to a wide frequency range.

The following are suggestions to improve both the FEM model and the EXP setup for future research. For the FEM model, the first step is to improve the accuracy of the geometry in the FEM simulation. In addition, the measurement of dimensions of the EXP setup should be conducted using more precise equipment. Currently, the calibration function employs linear interpolation to predict the difference between the FEM and EXP frequency responses. This calibration function can be improved to use nonlinear interpolation. The samples are numerically simulated as nondispersive material in the FEM model. This approximation has been used as an effort to minimize the computational cost of the FEM simulation. In the future, the FEM can be modified to model the dispersive dielectric behavior of materials within a wider range of frequency in a reasonable amount of time.

In the EXP model, the imperfections of the sensor should be eliminated and avoided as possible. Examples of these imperfections are the warped LTCC sheet and disjointed silver-epoxy paints on the LTCC sheets. The most practical improvement is to increase the amplitude of EM signals. This increase may amplify the signal-to-noise ratio where the instrument's noise remains constant. Consequently, the gradient of EM waves can be used to induce dielectrophoretic forces and displace the suspended particles toward the receiver in order to enhance the discriminating signal. In other words, a receiver can be added to the setup at the location toward which the particles are pushed. This innovation can lead to improving the measurements sensitivity.

REFERENCES

Agilent (2008). "Agilent Solutions for Measuring Permittivity and Permeability with LCR Meters and Impedance Analyzers." Application Note 1369-1, Agilent Technologies Inc., *Agilent literature number 5980-2862EN*, US, 27 pgs.

Azad, M., H.D.O. Sangrey, A. Farid, J. Browning, and E. Barney Smith (2013). "Electromagnetic Stimulation of Two-Phase Transport in Water for Geoenvironmental Applications," *ASTM, Geotechnical Testing Journal*, 36(1), 97-106.

Blackham, D.V., and R.D. Pollard (1997). "An improved technique for permittivity measurements using a coaxial probe." *Instrumentation and Measurement*, IEEE Transactions, 46(5), 1093-1099.

Bolvardi, V. (2014). "Electromagnetically induced contaminant removal" MSc thesis, Department of Civil Engineering, Boise State University, Boise, Id, 98 pgs.

Farag, A.M., and D.D. Harper (2014). "A review of environmental impacts of salts from produced waters on aquatic resources." *International Journal of Coal Geology*, U.S. Geological Survey, Jackson, WY, 126, 157-161.

Jilani, M.T., M. Z. Rehman, A. B. Khan, M. T. Khan, and M. Ali (2012). "A brief review of measuring techniques for characterization of Dielectric Materials." *ITEE Journal*, 1(1), 1-5.

Jouyban, A., S. Soltanpour, and H.K. Chan (2004). "A simple relationship between dielectric constant of mixed solvents with solvent composition and temperature" *International Journal of Pharmaceutics*, 269(2004), 353-360.

Kaatze, U. (2013). "Measuring the dielectric properties of materials. Ninety-year development from low-frequency techniques to broadband spectroscopy and high-frequency imaging." *Journal of Measurement Science and Technology*, AAAS, 24(012005), 31 pgs.

Kheir, M. S., H. F. Hammad, and A. Omar (2008). "Measurement of the dielectric constant of liquids using a hybrid cavity-ring resonator." *PIERS Proceedings*, Cambridge, USA, 566-569.

Komarov, V., S. Wang, and J. Tang (2005). "Permittivity and Measurements," *Encyclopedia of RF and Microwave Engineering*, K. Chang, eds., John Wiley and Sons, Inc., 3693-3711.

Lamkaouchi, K., A. Balana, G. Delbos, and W. J. Ellison (2003). "Permittivity measurements of lossy liquids in the range 26-110 GHz," *Measurement Science and Technology*, Institute of Physics, 14, 444-450.

Nair, K.M. (2013). "Low temperature co-fired ceramics (LTCC)-based electronic circuit materials for high frequency applications." *DuPont Electronic Technologies Seminar*, Materials Science and Engineering Department, Boise State University, Boise, Id.

Peyman, A., C. Gabriel, Grant EH (2007). "Complex permittivity of sodium chloride solutions at microwave frequencies." Bioelectromagnetics 28, Wiley-Liss, Inc., 264–274.

Piercenet (2014). "Bovine Serum Albumin (BSA) Standards," Internet: http:// www.piercenet.com/product/bovine-serum-albumin-bsa-standards. Accessed 10/20/14.

Tereshchenko, O.V., F.J.K. Buesink, and F.B.J. Leferink (2011). "An overview of the techniques for measuring the dielectric properties of materials." *IEEE General Assembly and Scientific Symposium*, *Proceedings of the 2011 XXXth URSI*, 1-4.

USGS (2012). "Pesticides in groundwater," Internet: http://water.usgs.gov/edu/pesticidesgw.html. Accessed 10/20/14.

Von Hippel, A.R. (1954). *Dielectric Materials and Applications*. The Technology Press of M.I.T. and John Wiley & Sons, New York, 290 pgs.

Wang, P., and A. Anderko (2001). "Computation of dielectric constants of solvent mixtures and electrolyte solutions." *International Journal of Fluid Phase Equilibria*, 186, 103-122.

Wentworth, S. M. (2005). *Fundamentals of Electromagnetics with Engineering Applications*, Wiley & Sons, New York, 274 pgs.

Xie, C., G. Segeral, G. Roux, and P. Hammond (2004). "Methods and apparatus for estimating on-line water conductivity of multiphase mixtures." *U. S. Patent 6,831,470*, Schlumberger Technology Corporation, Ridgefield, Ct, 29 pgs.